Available online at www.sciencedirect.com
SCIENCE DIRECT®
Journal of Nuclear Materials 323 (2003) 243–250
journal of nuclear materials
www.elsevier.com/locate/jnucmat

MD and KMC modeling of the growth and shrinkage mechanisms of helium–vacancy clusters in Fe

K. Morishita [a,*], R. Sugano [a], B.D. Wirth [b]

[a] *Institute of Advanced Energy, Kyoto University, Gokasho, Uji, Kyoto 611-0011, Japan*
[b] *Lawrence Livermore National Laboratory, Livermore, CA 94551, USA*

Abstract

A multiscale modeling approach, which is based on atomistic simulations, was applied to investigate the growth and shrinkage mechanisms of helium–vacancy (He–V) clusters in Fe. Firstly, a molecular dynamics technique with empirical interatomic potentials was used to determine energies for the formation and dissociation of clusters as a function of their size and He density. Both the number of He atoms and vacancies in a cluster ranged from 0 to 20. The dissociation energy of clusters showed a strong dependence on the He density, rather than the cluster size, indicating that the growth and shrinkage of clusters strongly depend on the He density. Secondly, these dissociation energies were employed in a kinetic Monte-Carlo (KMC) simulation, to explore long-time cluster behavior. The KMC simulation indicated that He can stabilize He–V clusters by suppressing thermal vacancy emission and by promoting thermal self-interstitial Fe atom emission. A preliminary KMC simulation to investigate the migration behavior of He–V clusters is also presented.
© 2003 Elsevier B.V. All rights reserved.

PACS: 61.80.Az; 61.72.−y; 61.72.Cc; 61.72.Qq

1. Introduction

During the operation of fusion reactors, He is directly implanted or generated internally by (n,α) nuclear transmutation reactions in materials, concurrently with energetic displacement damage. High He concentrations and the formation of He bubbles in materials are known to enhance void swelling, cause intergranular embrittlement, and produce surface roughening and blistering. This degradation results from the fact that He is insoluble and therefore tends to precipitate into vacancy clusters or voids in materials.

Trinkaus has classified helium–vacancy (He–V) clusters and He bubbles into three characteristic size classes: atomistic bubble nucleus, nonideal gas bubbles and ideal gas bubbles [1]. The lowest size class is usually indicated by He_nV_m clusters, which may play an important role in the nucleation of He bubbles. However, a physically precise description of bubble nucleation and the transformation of clusters into bubbles have not yet been obtained. The objective of the present study is to provide an appropriate model for nucleation and growth of He bubbles by using a multiscale modeling approach, where the advantages of various simulation techniques are utilized to understand the physical phenomena that take place at a wide variety of time and length scales. As a first step toward the establishment of the model, molecular dynamics (MD) was employed to investigate the energetics of He–V clusters in Fe, and then, a kinetic Monte-Carlo (KMC) technique was applied to understand the thermal stability and migration behavior of the clusters. To validate the computational results, the calculated energies were directly compared with experimental measurements using thermal He desorption spectrometry (THDS).

* Corresponding author. Tel.: +81-774 38 3477; fax: +81-774 38 3479.
E-mail address: morishita@iae.kyoto-u.ac.jp (K. Morishita).

0022-3115/$ - see front matter © 2003 Elsevier B.V. All rights reserved.
doi:10.1016/j.jnucmat.2003.08.019

2. MD calculation of formation energies

In order to evaluate the formation energies of defect clusters in Fe, the empirical interatomic potentials developed by Ackland et al. [2], Wilson and Johnson [3], and Beck [4] were employed to describe interactions between Fe–Fe, Fe–He and He–He, respectively. The Beck potential was modified to smoothly connect with the Ziegler–Biersack–Littmark (ZBL) potential [5] that is appropriate at short atomic separation. Computational box size was $10a \times 10a \times 10a$, where a is the lattice constant of Fe. Periodic boundary conditions were applied. Details of the calculation method are described in Ref. [6].

The formation energies of vacancy clusters (void) and self-interstitial atom (SIA) clusters in bcc Fe were calculated as a function of cluster size and shape, and the size dependence of the lowest formation energies are well described by the following equations, respectively:

$$E_f(V_k) = 2.7906k^{2/3} - 0.75526k^{1/3}, \quad (1)$$

$$E_f(I_k) = 1.1392k + 4.7035k^{1/2}, \quad (2)$$

where $E_f(V_k)$ is the formation energy of the cluster of k vacancies, and $E_f(I_k)$ is the formation energy of the cluster of k SIAs. The cluster size, k, investigated here ranged up to 76 and 25 for the vacancy and SIA clusters, respectively. The vacancy cluster formation energy agrees very well with a continuum level equation describing void surface energy, down to as small as one vacancy [7]. The binding energy of the vacancy and SIA clusters was defined as follows:

$$E_b(j_k) = E_f(j_1) + E_f(j_{k-1}) - E_f(j_k), \quad (3)$$

where j is V or I. Both the binding energies defined in this way show an increasing function of cluster size. In addition, as shown in Fig. 1 of Ref. [6], the binding energy of SIA clusters is greater than that of vacancy clusters at any size, indicating that a vacancy cluster is thermally less stable than an SIA cluster. In fact, even for larger size, the binding energy of vacancy clusters does not take more than about 1.2 eV, while the binding energy of SIA clusters is greater than 2.0 eV even for 4 SIAs. However, when He atoms are introduced into vacancy clusters, the binding state of the clusters is dramatically changed, as mentioned in the next section.

The formation energy of a He–V cluster that contains n He atoms and m vacancies was defined as follows:

$$E_f(\mathrm{He}_n\mathrm{V}_m) = E_{tot}(\mathrm{He}_n\mathrm{V}_m) - \{n\varepsilon_{He} + (N-m)\varepsilon_{Fe}\}, \quad (4)$$

where $E_{tot}(\mathrm{He}_n\mathrm{V}_m)$ is the calculated total energy of a computational cell containing a $\mathrm{He}_n\mathrm{V}_m$ cluster, ε_{Fe} is the cohesive energy of a perfect bcc Fe crystal, and ε_{He} is the cohesive energy of a perfect fcc He crystal. ε_{Fe} and ε_{He} was calculated to be −4.316 and −0.00714 eV/atom, respectively. N denotes the number of perfect bcc lattice sites in the computational cell and therefore $(N-m)$ is the number of Fe atoms in the cell. From the formation energy obtained here [7], the binding energies of various point defects to a $\mathrm{He}_n\mathrm{V}_m$ cluster were calculated, where n and m ranged from 0 to 20. The binding energy of a vacancy, an interstitial He atom, and a self-interstitial Fe atom to $\mathrm{He}_n\mathrm{V}_m$ clusters was calculated according to the following equations, respectively:

$$E_b(V) = E_f(V) + E_f(\mathrm{He}_n\mathrm{V}_{m-1}) - E_f(\mathrm{He}_n\mathrm{V}_m), \quad (5)$$

$$E_b(\mathrm{He}) = E_f(\mathrm{He}) + E_f(\mathrm{He}_{n-1}\mathrm{V}_m) - E_f(\mathrm{He}_n\mathrm{V}_m), \quad (6)$$

$$E_b(I) = E_f(I) + E_f(\mathrm{He}_n\mathrm{V}_{m+1}) - E_f(\mathrm{He}_n\mathrm{V}_m). \quad (7)$$

The formation energy of an isolated vacancy ($E_f(V)$), an interstitial He atom ($E_f(\mathrm{He})$) and an isolated self-interstitial atom (SIA) ($E_f(I)$) in bcc Fe was calculated to be 1.70, 5.25 and 4.88 eV, respectively. The binding energy defined in this way exactly equals the difference in total energy before and after the interaction between such a point defect and a He–V cluster. For example, from Eqs. (4) and (5), the vacancy binding energy is rewritten by

$$E_b(V) = \{E_{tot}(V) + E_{tot}(\mathrm{He}_n\mathrm{V}_{m-1})\} - \{E_{tot}(\mathrm{perfect}) + E_{tot}(\mathrm{He}_n\mathrm{V}_m)\}, \quad (8)$$

where $E_{tot}(\mathrm{perfect})$ is the total energy of a perfect crystal containing N Fe atoms which can be expressed as $N\varepsilon_{Fe}$, and $E_{tot}(V)$ is the total energy of a crystal containing an isolated vacancy with $(N-1)$ Fe atoms. Thus, Eq. (8) shows a difference in total energy between the crystal of $2N$ lattice sites containing a $\mathrm{He}_n\mathrm{V}_m$ cluster and the same size of a crystal containing both a $\mathrm{He}_n\mathrm{V}_{m-1}$ cluster and an isolated vacancy.

Extension of Eq. (7) provides the definition of the binding energy of an SIA cluster to $\mathrm{He}_n\mathrm{V}_m$ clusters, as follows:

$$E_b(I_k) = E_f(I_k) + E_f(\mathrm{He}_n\mathrm{V}_{m+k}) - E_f(\mathrm{He}_n\mathrm{V}_m), \quad (9)$$

where $E_f(I_k)$ is the formation energy of the cluster of k SIAs, which can be fitted to Eq. (2).

3. Binding energy of He–V clusters

Fig. 1 shows a plot of the binding energies versus the He density of clusters in bcc Fe. The He density was defined as the helium-to-vacancy ratio of clusters, which was the number of He atoms divided by the number of vacancies in the cluster. Namely, the He density of a $\mathrm{He}_n\mathrm{V}_m$ cluster was provided by n/m. As shown in the figure, the binding energies primarily depend on the He density. The cluster size dependence of the binding en-

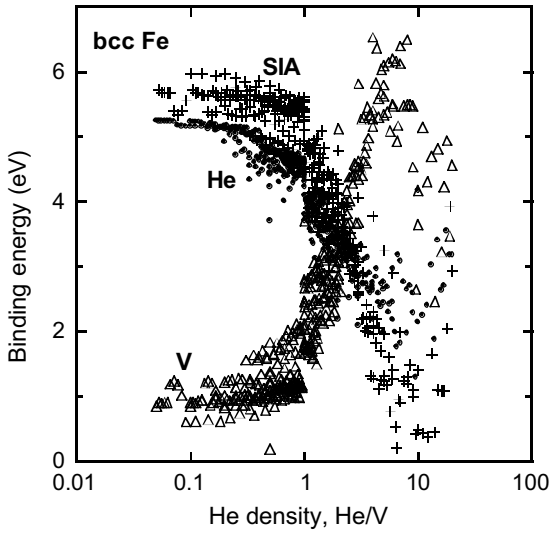

Fig. 1. The binding energy of a vacancy, an interstitial He atom, and an SIA to He–V clusters in bcc Fe as a function of the He density of clusters. All the binding energies strongly depend on the He density, rather than cluster size.

ergies is relatively small, except for He_nV_1 clusters, where the binding energies of a vacancy and an SIA are somewhat greater and the binding energy of an interstitial He atom is somewhat lower to the He_nV_1 clusters than to He_nV_m clusters.

Except for the extremely high He density regime (>6 He/V), the binding energy of a vacancy to He–V clusters gradually increases with increasing He density, which is consistent with the conclusion provided by Adams and Wolfer [8]. The calculated binding energy of a vacancy to high-density He–V clusters surprisingly exceeds 6 eV, implying that, at any temperature, a vacancy cannot be detrapped from the cluster. Such a high binding energy is inconsistent with the report for He in Ni [9], where Sharafat et al. have extrapolated and evaluated the binding energy of a vacancy to small He–V clusters, from the rather macroscopic point of view. This inconsistency may result from the fact that their estimation was only based on force balance between bubble surface tension and gas pressure, and moreover, the gas pressure was evaluated using the He equation of state (EOS) where only He–He interaction was considered. For such small clusters as investigated here (the number of He and vacancies ranged from 0 to 20), the interaction of He atoms with surrounding metal atoms is more important than the interaction between He–He in the cluster and therefore the metal–He interaction cannot be ignored. Our atomistic calculations giving such high values of the vacancy binding energy may indicate that there is a difficulty in determining the energies of small clusters from the macroscopic point of view. A physical description connecting our atomistic evaluation for smaller clusters and their macroscopic evaluation for larger clusters is beyond the scope of the present work, but it is very important and should be done in the future.

The configuration of He atoms in a He–V cluster strongly depends on the He density of the cluster. When the helium-to-vacancy ratio is approximately 1, the He atoms have bcc configuration, coherent with matrix Fe lattice atoms. On the other hand, when the ratio is greater than approximately 6, they have close-packed configuration in the cluster, and, in this case, the collective motion of He atoms in the cluster produces bubble pressure large enough to push a Fe atom off from its normal site and spontaneously creates additional vacancies and associated SIAs, thereby lowering the He density. These results indicate that the maximum He-to-vacancy ratio is about 6. The SIAs produced in high He density clusters were bound to the cluster, and moreover, the SIAs agglomerated on the same side of the cluster rather than uniformly distributed over the cluster surface, which is consistent with Wilson's observations [10]. This athermal behavior may effectively increase the number of vacancies in the cluster, and therefore, reduce the actual He density of the cluster. This may reflect the vacancy binding energy curve in Fig. 1, where the dependence of the binding energy on the He density changes when the ratio is greater than about 6. For example, as shown in Fig. 1, the binding energy of a vacancy to clusters of He-to-vacancy ratio 10 is approximately the same as that of ratio 3, indicating that the He density of the clusters is effectively reduced from 10 to 3 because of athermal vacancy creation.

The employed interatomic potentials used in this study show that the repulsive interaction between Fe–He is much greater than the relatively weak He–He interaction of a closed shell noble gas. It results in the energetically favorable He clustering in Fe through a decrease in the number of high energy, repulsive Fe–He interactions. This is a possible reason why He atoms make a cluster in Fe, though the cohesive energy of He atoms is negligibly small ($\varepsilon_{He} = -0.00714$ eV/atom for fcc He). In the same way, He atoms prefer to be bound to vacancies for further reduction in the number of the Fe–He interactions. In fact, He atoms are strongly trapped by vacancies and vacancy clusters, and namely, the binding energy of an interstitial He atom to nearly empty voids is very high. Fig. 1 also shows the binding energies of an interstitial He atom to He–V clusters as a function of the He density. The binding energy of an interstitial He atom to He–V clusters decreases from approximately the same value as interstitial He formation energy ($E_f(He) = 5.25$ eV) at 0 He/V to the value slightly smaller than 2 eV at 6 He/V, followed by an increase at ratios greater than 6. The change in the dependence of the energies on the He density at greater than 6 He/V may be because of the 'athermal SIA production and associated effective decrease in the He

density', which is the same reason for the change of the dependence of vacancy binding energy on the He density, as mentioned above. The decreasing and increasing behavior of the He binding energy is qualitatively consistent with the results of He in Ni reported by Wilson et al. [10].

Fig. 1 also shows the binding energy of an SIA to He–V clusters as a function of the He density. Similar to the density dependence of the He binding energy, the binding energy of an SIA to He–V clusters also decreases from the value close to the Frenkel pair formation energy ($E_f(V) + E_f(I) = 1.70 + 4.88 = 6.58$ eV) at 0 He/V, to nearly zero eV at 6 He/V, followed by an increase with increasing the He density. The density dependence of the SIA binding energy is also qualitatively consistent with Wilson's calculations [10]. It should be noted here that the SIA binding energy is almost zero at high densities. The cluster is fully occupied by 6 He atoms per a vacancy and therefore additional incoming SIAs are prevented from recombining with vacancies.

The binding energies obtained above clearly show some of the He effects on the thermal stability of He–V clusters in Fe during and after irradiation. One is the impact on the binding energy of a vacancy to He–V clusters, where the vacancy binding energy increases with the He density. The second is the impact on the binding energy of an SIA to He–V clusters, where the SIA binding energy decreases with the He density. Both effects will stabilize He–V clusters. In order to profoundly understand He effects, the binding energies of He–V clusters were compared with those of copper–vacancy (Cu–V) clusters in Fe [6], where a Cu atom is usually a substitutional impurity in Fe. It should be noted that the notation of a Cu_nV_m cluster and the definition of the Cu density of the cluster, n/m, were, on purpose, set to be the same as those for He–V clusters, though such notation is not usual for substitutional impurities. In Cu–V clusters, the athermal production of SIAs takes place at copper-to-vacancy ratios greater than 1, which may reflect the fact that an effective pair potential value of the employed Fe–Fe potential is lower than that of FeCu at the atomic separations expected here. The critical value of 1 for Cu–V clusters may correspond to the critical value of 6 for He–V clusters, and the difference in the critical values may be explained by the difference in the size of the impurities in Fe. In the case of He–V clusters, the gradual but significant changes in the binding energies of a vacancy and an SIA to the clusters were observed for the He density up to the critical value, while such drastic changes were not observed for Cu–V clusters. Thus, the drastic changes in binding energies are one of the characteristic features of He effects in Fe. Further investigation of binding states for other impurity–vacancy clusters in Fe is interesting and it may be required as a reference to understand the He effects more deeply.

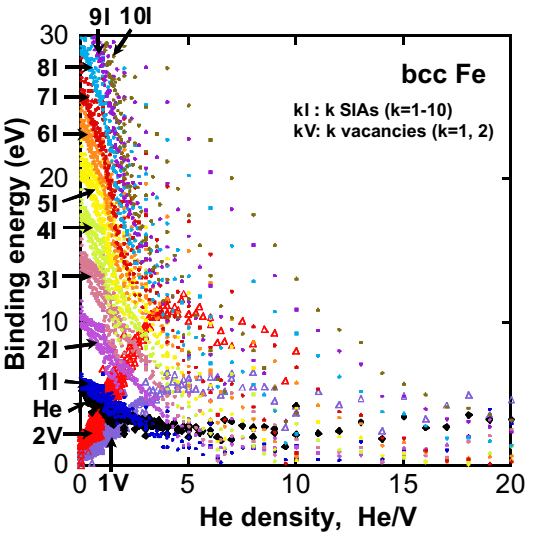

Fig. 2. The binding energy of an SIA cluster to He–V clusters in bcc Fe as a function of the He density of He–V clusters. The SIA cluster binding energy for the He–V clusters of high He density is significantly low.

Fig. 2 shows the binding energy of an SIA cluster to He–V clusters as a function of the He density, which was calculated using Eq. (9). The binding energy primarily depends on the He density rather than cluster size, but there is also the difference of the density dependence between He_nV_1 clusters and He_nV_m ($m \neq 1$) clusters. Interesting is the relatively higher density regime, where the binding energy of an SIA cluster to He–V clusters is very small, indicating that the emission of an SIA cluster from the clusters, i.e., 'loop punching [11]', can take place even at relatively lower temperatures.

4. Dissociation energy of He–V clusters

The frequency of dissociation of a defect j from a He–V cluster is usually described by the following equation [15,16]:

$$v(j) = v_0 \exp(-E_D(j)/kT), \tag{10}$$

where j denotes a defect that dissociates from a He–V cluster, i.e., j = V, He, SIA, SIA cluster, etc. v_0 is the attempt frequency that is usually assumed to be 10^{13} s^{-1}, k is the Boltzman constant, and T is temperature. $E_D(j)$ is the dissociation energy that is defined as follows [6,16,17]:

$$E_D(j) = E_b(j) + E_m(j), \tag{11}$$

where $E_b(j)$ is the binding energy of point defect j to a He–V cluster. $E_m(j)$ is the activation energy for migra-

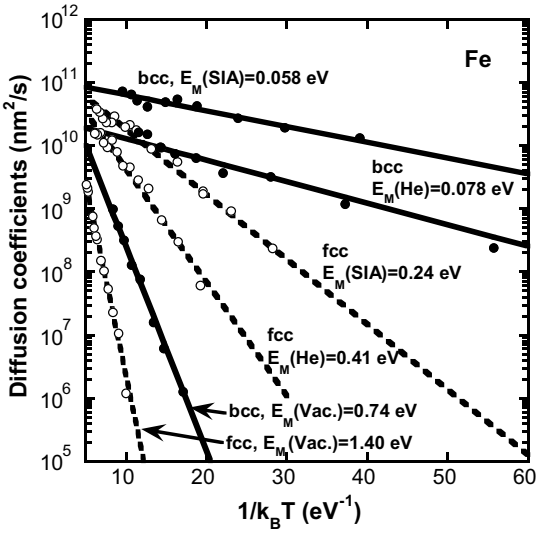

Fig. 3. The Arrhenius plot of diffusion coefficients of a vacancy, an interstitial He atom and an SIA in bcc and fcc Fe. The diffusion coefficients were calculated from the trajectories of the point defects during 1–100 ns at various temperatures. The slope of the plot provides the migration energy of the point defects.

tion of point defect j. These were calculated to be 0.74, 0.078 and 0.058 eV for $j = \mathrm{V}$, He, SIA in bcc Fe, respectively, where the migration energies were obtained by the slope of the Arrhenius plot of diffusion coefficients calculated from the trajectories of the defects during 1–100 ns at various temperatures, as shown in Fig. 3.

Fig. 4 shows the dissociation energies of a vacancy, an interstitial He atom and an SIA from He–V clusters as a function of the He density of clusters. The figure provides a deep insight into the growth and shrinkage behavior of He–V clusters in Fe during post-He-irradiation annealing, from the viewpoint of energetics. At a particular annealing temperature, it is generally expected that, if the activation energy for a certain dissociation process is lower than kT, then the dissociation process can take place. When temperature gradually increases during post-irradiation annealing, firstly, at lower temperatures, thermal SIA emission can take place from clusters of high He density, and then, at higher temperatures, He can dissociate from clusters of higher He density, as well as thermal vacancy emission from the clusters of lower He density. It is interesting to note that, when thermal SIA emission takes place from a He–V cluster, the He density of the cluster decreases because of an increase in the number of vacancies. In the same way, when He dissociation takes place, the He density is decreased by a decrease in the number of He atoms in the cluster. Moreover, when thermal vacancy emission takes place, the He density increases due to a decrease in the number of vacancies in the cluster. Consequently, the He density of stable He–V clusters is given by the region below each curve in Fig. 4. For example, when the annealing temperature corresponds to the dissociation energy of 2 eV, the He density of stable clusters lies roughly from 0.7 to 4. At higher temperature, the lowest limit of the He density gradually increases and the highest limit gradually decreases. Finally, when the temperature corresponds to about 3.6 eV, the He density of stable clusters can only be 1.8, at which all the dissociation energy curves intersect in the figure. Furthermore, when the temperature increases more, the He density of clusters is still about 1.8. In this way, dissociation of a vacancy, He and an SIA from He–V clusters strongly depend on the He density of the cluster and the

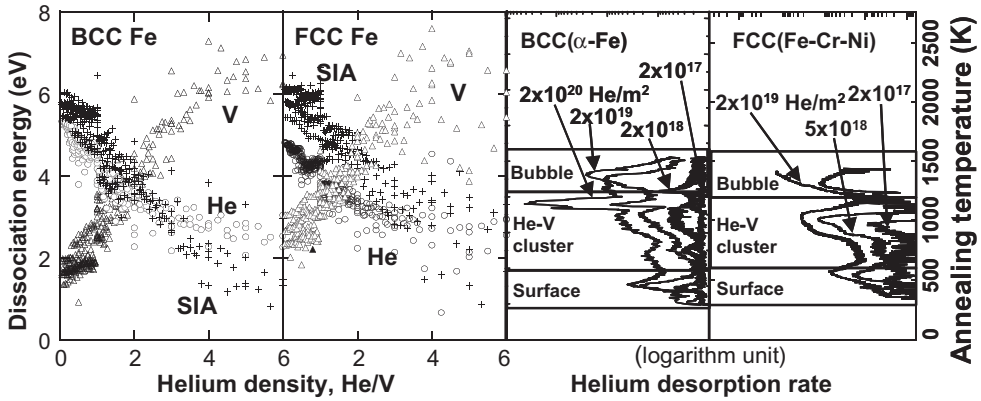

Fig. 4. The calculated dissociation energies of a vacancy, an interstitial He atom and an SIA from He–V clusters in bcc and fcc Fe as a function of the He density of clusters. The calculated energies can be compared with experimental He desorption spectra obtained during the post-He-irradiation annealing at the linear ramping rate of temperature, 1 K/s. The relationship between the calculated dissociation energy and the annealing temperature is described by $E_D = 0.0029T$, where E_D is dissociation energy in eV and T is annealing temperature in K.

He density of stable He–V clusters can be determined by annealing temperature. It should be noted that the picture of dissociation processes discussed above does not include the effect of thermal vacancies nor other incoming defects.

5. Experimental validation

The calculated dissociation energy of an interstitial He atom from He–V clusters was directly compared with the experimental measurements of thermal He desorption spectrometry (THDS), where He atoms desorbed from Fe samples were detected as a function of annealing temperatures by a quadruple mass analyzer (QMA) during post-irradiation annealing at the constant temperature ramping rate of 1 K/s. All He atoms implanted were retained in the as-irradiated samples and all the He atoms were desorbed during the post-irradiation annealing. Details of the experiments are described in Ref. [12–14]. The THDS spectra roughly indicated that He atoms are dissociated from the surface at lower temperatures, from He–V clusters at intermediate temperatures (700–1200 K), and from bubbles (i.e., bubble migration) at higher temperatures.

When the temperature ramping rate is assumed to be 1 K/s that is the same as our experimental condition and the attempt frequency is assumed to be 10^{13} s^{-1}, the first-order reaction model [18] provides the calculated relationship between annealing temperature, T, in K and dissociation energies, E_D, in eV as $E_D = 0.0029T$ [6,15]. This is an equation describing the relationship between the present calculations and our experiments. Fig. 4 also shows a comparison between the calculated dissociation energy curves and the experimental THDS spectra. The ordinate in the figure of the energy curves corresponds to that in the figure of the THDS spectra through the relationship described above. From the dissociation energy curves, He atoms can be detrapped from stable He–V clusters at temperatures approximately from 700 to 1200 K, which is consistent with experimental observation. However, there is a problem with the comparison, because a phase transformation from bcc to fcc takes place in pure Fe at 1183 K. Therefore, the dissociation energies of He–V clusters in fcc Fe were also calculated using the same potential set as used in the calculations for bcc Fe. Although the Ackland potential for Fe–Fe interaction was developed so as to fit bcc Fe [2], it also reproduces the lattice constant of fcc Fe very well (the calculated lattice constant of fcc Fe is 0.3680 nm). In addition, the elastic constants for fcc Fe were calculated to be $C_{11} = 187$, $C_{12} = 122$ and $C_{44} = 98$ GPa at 0 K, which are consistent with the experimental elastic constants of $C_{11} = 154$, $C_{12} = 122$ and $C_{44} = 77$ GPa at 1428 K [19]. Since Fe–He and He–He interactions were described by purely pairwise interatomic potentials [3,4] and atom–atom separation is the most important parameter for energy evaluations, it may not be unreasonable that the potential set is also useful for evaluation of He–V clusters in fcc Fe. The dissociation energies for He–V clusters in fcc Fe is also plotted in Fig. 4. The dependence of the energies for fcc Fe on the He density is similar to the case for bcc Fe, but the magnitude of the dissociation energy of an interstitial He atom from He–V clusters in fcc Fe is somewhat smaller than that in bcc Fe. This may indicate that, when the phase transformation takes place from bcc to fcc, the He binding strength of the clusters suddenly decreases, resulting in dissociation of excess He. In fact, a burst of He desorption from α-Fe was experimentally observed at around the phase transformation temperature, at which the He desorption peak is so sharp that the usual first-order dissociation model cannot explain the peak. Such a peak is not observed in an fcc Fe (Fe–Cr–Ni alloy), where no phase transformation takes place. Thus, our calculations indicate athermal He desorption at the phase transformation temperature, which is consistent with experimental observations. Helium desorption accompanied with the phase transformation was also discussed in Ref. [14] purely from an experimental point of view.

6. Lifetime of He–V clusters

An MD simulation technique is a useful tool for physical description of the static and dynamic behaviors of nano-scale defects in materials. However, the simulation time is limited within about 1 μs even when using recent high performance computers. The lifetime of He–V clusters may depend on their size and He density and temperature, and it could be, in many cases, beyond the limitation. Therefore, a KMC technique was employed to evaluate the lifetime of He–V clusters, where only phenomenological 'known' events are considered. The KMC simulation includes the events of dissociation of a vacancy, an interstitial He atom and an SIA from He–V clusters, but, at present, for simplicity, it does not include the dissociation of an SIA cluster. The occurrence probabilities of the events were assumed to be proportional to Eq. (10). Only the vacancies, He atoms and Fe atoms located at cluster-matrix interface were assumed to be the candidates for dissociation. Energetics associated with these events was described by the MD results mentioned above. The time step employed in the calculations is $\Delta t = -\log(R)/\Sigma\nu_i$, where R is random number from 0 to 1 and ν_i is the occurrence probability of an event i [20].

Fig. 5 is the time evolution of the size of a He–V cluster in bcc Fe as a function of its initial He density, where cluster size is defined as the number of vacancies in the cluster, independent on the number of He atoms.

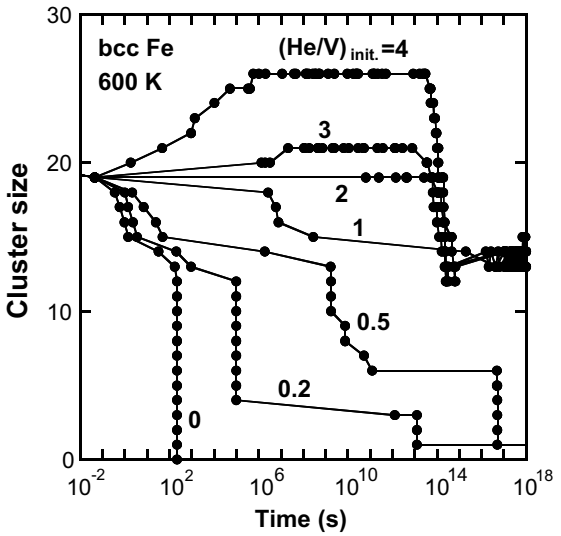

Fig. 5. The time evolution of the size of He–V clusters in bcc Fe as a function of the initial He density of clusters. Initial cluster size is 20 vacancies and temperature is 600 K.

Initial cluster size is 20 and temperature is fixed at 600 K. Without He atoms, cluster size rapidly decreases and the cluster is completely collapsed within 10^2 s due to thermal vacancy emission. However, when the initial He density increases, cluster lifetime dramatically increases. In addition, when the initial He density is greater than 2, the cluster size increases initially due to thermal SIA emission. Thus, the time development of cluster size, or cluster lifetime, strongly depends on the initial He density. It is noted that the cluster lifetime evaluated here shows the thermal stability of an isolated He–V cluster solely as the general nature of the cluster. Namely, it does not include the effect of incoming defects produced by irradiation. Such an effect may be significant, but introduction of the effect has no general results because how frequently the radiation-induced defects come to He–V clusters strongly depends on irradiation condition and microstructures such as dislocations, grain boundaries, etc. Evaluation of cluster lifetime for the individual specific irradiation and microstructure conditions is beyond the scope of the present paper.

7. Preliminary calculation of He–V cluster migration

The migration behavior of He–V clusters in bcc Fe was investigated by KMC calculations, where the effect of thermal vacancies and the diffusion of Fe atoms on the cluster surface were included as well as the dissociation events mentioned above. The thermal vacancy effect and the surface migration of Fe atoms are described by the following equations, respectively:

$$v = v_0 \exp[-(E_f(V) + E_m(V))/kT], \tag{12}$$

$$v = v_0 \exp[-(E_M + \Delta E)/kT], \tag{13}$$

where $E_f(V)$ is vacancy formation energy and $E_m(V)$ is vacancy migration energy. The vacancy formation and migration energies are 1.70 and 0.74 eV obtained by MD calculations, respectively. The present model description of the surface Fe atom diffusion was similar to the work by Huang et al. [21]. Both E_M and ΔE were assumed to be a function of the He density and the coordination number, where the coordination number is defined as the number of Fe atoms within the first nearest neighbor distance from the Fe atom in considering. ΔE is the difference between the potential energies of a Fe atom at positions before and after a possible jump. The atom potential energy was obtained by MD calculations as a function of the coordination number and the He density. On the other hand, E_M is temporarily assumed to be the same as the migration energy of a Fe atom on a flat free surface (without He). Details of the simulation methods and further work will be reported elsewhere [22].

Inclusion of the effects of Fe atom migration on the cluster surface and the existence of thermal vacancies into the KMC model provides an insight into the migration behavior of He–V clusters. The Arrhenius plot of diffusion coefficients of He–V clusters shows that the activation energy of He–V cluster migration is approximately the same as the migration energy of Fe atoms on the cluster surface, $E_M + \Delta E$. When 0.5–0.7 eV was used as E_M, the migration energy of a $He_{20}V_{20}$ cluster is approximately 0.89 eV [22]. It may indicate that cluster migration is dominated by the surface diffusion of Fe atoms, rather than by volume diffusion due to the effect

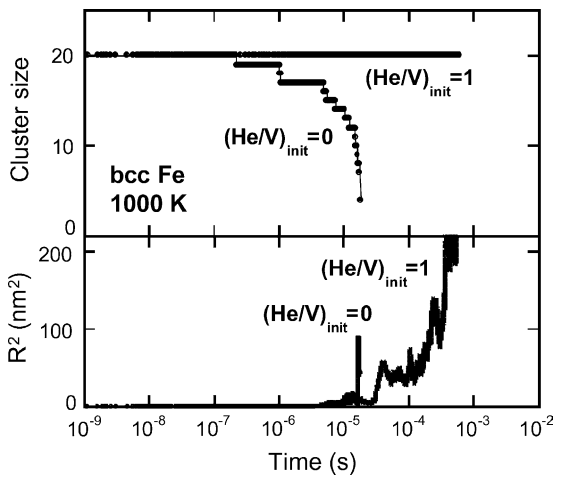

Fig. 6. The time development of the size and squared diffusion distance of He–V clusters in bcc Fe as a function of the He density. Initial cluster size is 20 vacancies and temperature is 1000 K.

of thermal vacancies. It should be noted that the prefactor of cluster diffusion coefficients is five orders of magnitude lower than that of usual point defect migration.

Fig. 6 shows the time development of the size and squared diffusion distance of clusters, as a function of the He density. Initial cluster size is 20, and temperature is fixed at 1000 K. When the He density is zero, cluster size gradually decreases with time due to thermal vacancy emission and cluster mobility increases with decreasing the size. On the other hand, when the He density is 1, cluster size does not change during the simulation time, and therefore, longer distance migration is available during longer cluster lifetime. Thus, cluster migration depends on the size and lifetime of clusters, both of which strongly depend on the He density.

8. Summary

The growth and shrinkage behaviors of He–V clusters in Fe were investigated by a multiscale modeling approach using MD and KMC techniques. He atoms in a He–V cluster can stabilize the cluster by suppressing vacancy emission and by promoting SIA emission, resulting in a drastic increase in the lifetime of the cluster. The thermal emission of a vacancy, an interstitial He atom and an SIA from He–V clusters greatly depend on the He density of clusters, rather than the cluster size. The preliminary KMC calculations were also performed to investigate the migration behavior of He–V clusters. The diffusion of a He–V cluster depends on the size and lifetime of the cluster, and therefore depends on the He density.

References

[1] H. Trinkaus, Radiat. Eff. 78 (1983) 189.
[2] G.J. Ackland, D.J. Bacon, A.F. Calder, T. Harry, Philos. Mag. A 75 (1997) 713.
[3] W.D. Wilson, R.D. Johnson, Rare gases in metals, in: P.C. Gehlen, J.R. Beeler Jr., R.I. Jaffee (Eds.), Interatomic Potentials and Simulation of Lattice Defects, Plenum, 1972, p. 375.
[4] D.E. Beck, Mol. Phys. 14 (1968) 311.
[5] J.P. Biersack, J.F. Ziegler, Nucl. Instrum. and Meth. 194 (1982) 93.
[6] K. Morishita, R. Sugano, B.D. Wirth, T.D. de la Rubia, Nucl. Instrum. and Meth. B 202 (2003) 76.
[7] K. Morishita, B.D. Wirth, T.D. de la Rubia, A. Kimura, in: Proceedings of the 4th Pacific Rim International Conference on Advanced Materials and Processing (PRICM4), The Japan Institute of Metals, Hawaii, USA, 2001, p. 1383.
[8] J.B. Adams, W.G. Wolfer, J. Nucl. Mater. 166 (1989) 235.
[9] S. Sharafat, N.M. Ghoniem, J. Nucl. Mater. 122&123 (1984) 531.
[10] W.D. Wilson, C.L. Bisson, M.I. Baskes, Phys. Rev. B 24 (1981) 5616.
[11] J.H. Evans, A. van Veen, L.M. Caspers, Radiat. Eff. 78 (1983) 105.
[12] K. Morishita, R. Sugano, H. Iwakiri, N. Yoshida, A. Kimura, in: Proceedings of the 4th Pacific Rim International Conference on Advanced Materials and Processing (PRICM4), The Japan Institute of Metals, Hawaii, USA, 2001, p. 1395.
[13] R. Sugano, K. Morishita, H. Iwakiri, N. Yoshida, J. Nucl. Mater. 307–311 (2003) 941.
[14] R. Sugano, K. Morishita, A. Kimura, Fus. Sci. and Techn. 44 (2003) 446.
[15] W.D. Wilson, M.I. Baskes, C.L. Bisson, Phys. Rev. B 13 (1976) 2470.
[16] K. Morishita, R. Sugano, B.D. Wirth, Fus. Sci. and Techn. 44 (2003) 441.
[17] N.M. Ghoniem, S. Sharafat, J.M. Williams, L.K. Mansur, J. Nucl. Mater. 117 (1983) 96.
[18] A.V. Fedorov, Evolution of point defect clusters during ion irradiation and thermal annealing, PhD thesis, Delft University of Technology, 2000, p. 25.
[19] J. Zarestky, C. Stassis, Phys. Rev. B 35 (1987) 4500.
[20] C.C. Battaile, D.J. Srolovitz, J.E. Butler, J. Appl. Phys. 82 (1997) 6293.
[21] H. Huang, G.H. Gilmer, T.D. de la Rubia, J. Appl. Phys. 84 (1998) 3636.
[22] K. Morishita et al., in press.